A diagram technique for coupling calculations in compact groups

1975 J. Phys. A: Math. Gen. 8 1021

(http://iopscience.iop.org/0305-4470/8/7/005)

J. Phys. A: Math. Gen., Vol. 8, No. 7, 1975. Printed in Great Britain. © 1975

A diagram technique for coupling calculations in compact groups

G E Stedman

Department of Physics, University of Canterbury, Christchurch 1, New Zealand

Received 23 December 1974, in final form 25 February 1975

Abstract. The well known graphical technique for angular momentum theory is adapted for application in compact groups, including crystal point groups. The adaptation has been kept to a minimum; for simple phase groups, not much modification is called for. Phase conventions and permutation matrices are included by following Butler's algebraic treatment. Irreducible tensor operators, their conjugate tensors and the analogy with Feynman diagrams are discussed.

1. Introduction

Graphical techniques in angular momentum recoupling theory were developed by Jucys, Levinson and Vanagas and have been modified and applied by many workers. Two particularly helpful accounts are those of Brink and Satchler (1968) and Sandars (1969), who give earlier references; among later references we mention Briggs (1971) and El-Baz and Castel (1972).

Coupling techniques and tensor operators for finite (and non-commutative) groups have been discussed by many authors. The book by Griffith (1962) has been of particular significance for solid state physics, and covers many crystal point groups (O, D_n). His tabulations of *n-jm* symbols have been extended by Harnung (1973) to the octahedral spinor group, and by Butler and Wybourne (1975) to the tetrahedral group. The subject had been plagued by problems regarding phase conventions which have only recently been resolved. We take Butler's (1974) review as definitive for our purposes. All phases and permutation effects will be incorporated in the diagram method.

A diagram technique for compact groups has already been developed by Agrawala and Belinfante (1968). We have made use of several of their rules, in particular, using a stub for a 2-*jm* symbol, and a dotted line for a multiplicity index. However there are sufficient points of contrast to warrant a separate development. Phase problems have been simplified since their work; we depict matrix elements rather than operators; our diagrams may be rotated and are much closer in appearance to the conventional R_3 diagrams. Hopefully, the relative lack of technicalities and the examples included will assist the reader to gain facility quickly. An example of a standard coupling calculation (proof of the Racah back-coupling relation) is included to illustrate the full machinery we develop. Since diagrams make heavy demands on space, we shall not normally reproduce the algebraic equivalent of our diagrams. Equation x of Butler (1974) and equation y of Sandars (1969) will be quoted as Bx, Sy throughout; Butler's to give the exact algebraic equivalent, Sandars' to give the analogous R_3 diagram.

2. Diagrams in elementary group theory

Consider a compact group G with elements g. A unitary irreducible representation (irrep) of G will be denoted by a Greek letter λ, and the components by the corresponding Latin letters l; the dimension $|\lambda|$ will also be represented by $\hat{\lambda} \equiv |\lambda|^{1/2}, \check{\lambda} = |\lambda|^{-1/2}$, following Sandars. Most of our notation will follow Butler (1974).

The representation matrix element, $\langle \lambda l | O_g | \lambda l' \rangle \equiv \lambda(g)_{ll'}$, will be represented by

(S4.1) $\lambda(g)_{ll'}$ $\leftrightarrow$ 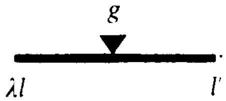

. (1)

Crudely speaking, the group operator O_g is represented by a solid triangle ('fulcrum'; we avoid the lines of Sandars (1969) and Agrawala and Belinfante (1968) since, with multiplicity lines and Feynman propagators, it would make for confusion) and the bra and ket states by solid lines. Strictly speaking the diagram may not be dissected; to be consistent with § 5 we should have to introduce a 2-*jm* symbol on the bra line even at this early stage.

Some general rules for diagram interpretation follow. All our diagrams may be rotated and mildly deformed, but not reflected. A vertex represents a matrix element or *n-jm* symbol. The order of suffices in the matrix element is given by working anticlockwise from the definitive symbol, in this case the triangle. A labelled solid line gives the relevant representation and component. Omitted labels are automatically summed over the group and representation respectively. The right side of equation (1) is thus unambiguous. The game we play is to invent diagram definitions which obey these rules, which are elegant, and which will unambiguously return the algebraic equations of Butler (1974).

Complex conjugation is indicated explicitly:

$(\lambda(g)_{ll'})^*$ $\leftrightarrow$ 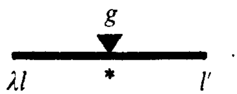

.

Group multiplication

(B2.8) 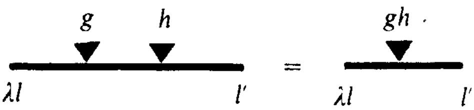

. (2)

and unitarity

(B2.6, 2.7)

(S4.2, 4.3)

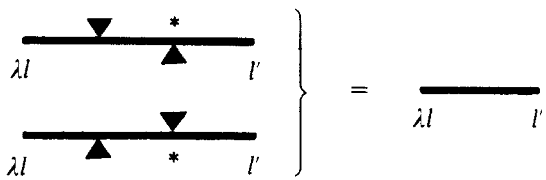

$(\delta_{ll'})$ (3)

are direct consequences of our rules.

By linking ends in equation (1) we introduce a $\delta_{ll'}$ factor; summing over l and l' gives the character:

$\chi^\lambda(g) \quad \leftrightarrow$ 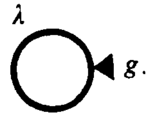 (4)

A simple closed loop labelled λ therefore has the value $\hat{\lambda}$.

A group integral ($|G|^{-1}\Sigma_g$ for a finite group) will be denoted by connecting the group operators to a solid circle, following Sandars (1968). The great orthogonality theorem becomes:

(B5.11)
(S4.5)

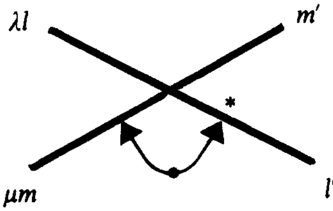 $=$ 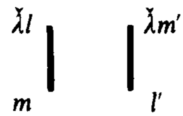 $\delta_{\lambda\mu}$. (5)

If $\mu = \mathbf{1}$ (the identity representation) we derive

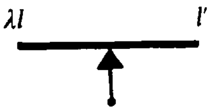 $= \quad \delta_{\lambda 1}(\delta_{l1}\delta_{l'1})$. (6)

Joining ends in equation (5) we obtain the character orthogonality theorem:

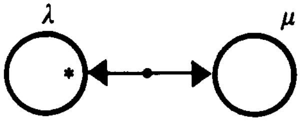 $=$  $\delta_{\lambda\mu} = \delta_{\lambda\mu}$. (7)

3. *n-jm* symbols

3.1. 3-jm symbol

The identity irrep **1** occurs just once in the Kronecker product $\lambda \otimes \lambda^*$; we may therefore define the multiplicity $n_{\lambda_1\lambda_2\lambda_3}$ ($\equiv R$) of the triple ($\lambda_1\ \lambda_2\ \lambda_3$) either as the number of times **1** occurs in $\lambda_1 \otimes \lambda_2 \otimes \lambda_3$ or the number of times λ_3^* occurs in $\lambda_1 \otimes \lambda_2$, etc. If, for all triples in a group, $R \leqslant 1$ (eg R_3) the group is *simply reducible*. In general, $R > 1$, and R sets of coupling coefficients are necessary for each triple. We label these by $r = 1, \ldots, R$ and define the diagram form:

(B5.3)
(S3.1)

$\begin{pmatrix} \lambda_1 & \lambda_2 & \lambda_3 \\ l_1 & l_2 & l_3 \end{pmatrix}^r \quad \leftrightarrow$ 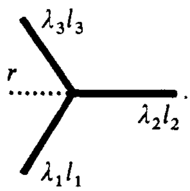 (8)

Complex conjugation (necessary for the tetrahedral group, for example) is represented explicitly. Note that all the rules in § 2 apply to this definition, the ordering being derived from the position of the multiplicity line.

A permutation $(\lambda_a\,\lambda_b\,\lambda_c)$ of the triple $(\lambda_1\,\lambda_2\,\lambda_3)$, $(abc) = \pi(123)$, will in general result in a new set of coupling coefficients

$$\begin{pmatrix} \lambda_a & \lambda_b & \lambda_c \\ l_a & l_b & l_c \end{pmatrix}^r$$

related to the old set by a matrix $\{\pi, \lambda_1\,\lambda_2\,\lambda_3\}_{rs}$. In R_3, where $R \leqslant 1$, the permutation matrix reduces, for cyclic permutations to unity and, for interchange permutations to a real phase of the form:

$$\{(12)\lambda_1\,\lambda_2\,\lambda_3\}_{rs} = (-1)^{j_1+j_2+j_3}\delta_{rs}. \tag{9}$$

It will prove to be elegant and convenient to avoid interchange permutations where possible by using twisted versions of the R_3 diagrams, especially in the general case when permutation matrices cannot be avoided.

One important result, equivalent to the unitarity of $\{\pi, \lambda_1\,\lambda_2\,\lambda_3\}_{rs}$, is

(B6.1) 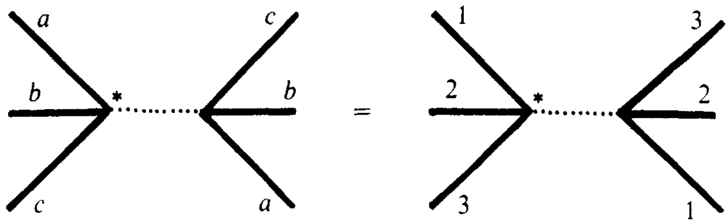

(9*a*)

where the omitted multiplicity index is summed and i represents $\lambda_i l_i$. Note that internal multiplicity lines will invariably connect the same triple in the same order. The following results appear naturally:

(B5.5)
(S3.12*b*) 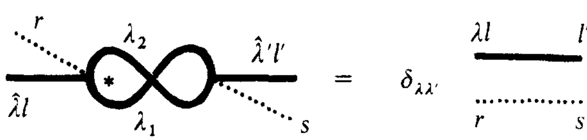

(10)

(B5.6)
(S3.12*a*) 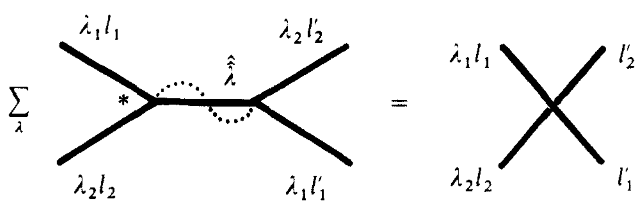

(11)

(B5.7)
(S4.4) 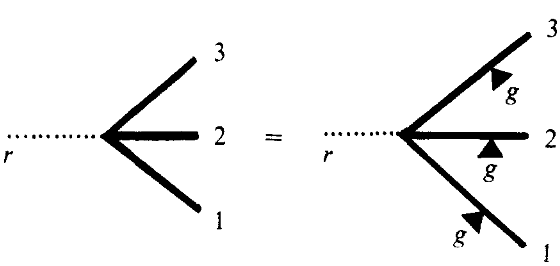

(12)

(B.5.12)

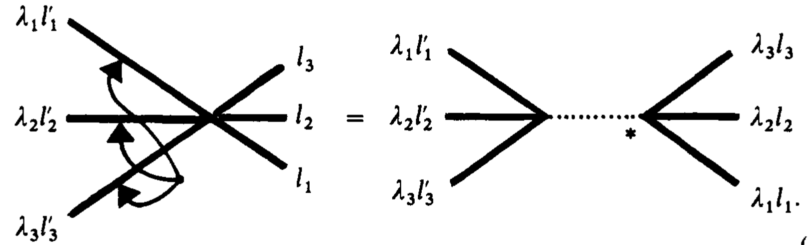

(13)

3.2. *Special cases*

If $\lambda_1 = \mathbf{1}$, the 3-*jm* symbol reduces to a unitary matrix that also relates $|\lambda l\rangle$ to $|\lambda^* l'\rangle$, called a 2-*jm* symbol (or 1-*j* coefficient):

(B5.10)
(S3.8)

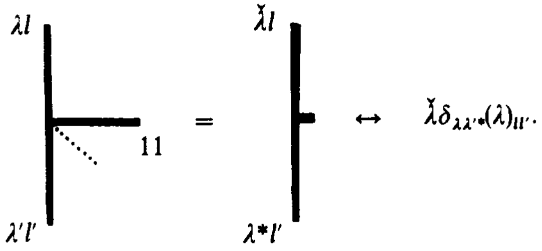

(14)

We prefer this stub representation to the (R_3) arrow representation; it emphasizes the connection with a 3-*jm* symbol and the difference in λl, $\lambda' l'$; note that if $\lambda \neq \lambda^*$ it matters which side of the stub we write λ. The reader who prefers arrows may simply replace

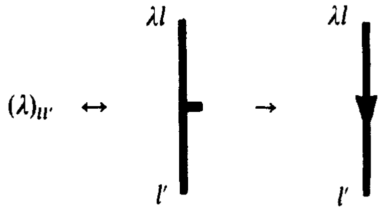

(15)

in all subsequent diagrams. In § 6 we show that the Feynman arrow on lines internal to a Feynman diagram has the same sense as the group-theoretical arrow of equation (15).

The 2-*jm* symbol may be chosen to be real (orthogonal), and of the form $(\lambda)_{ll'} = \delta_{ll'^*}$ ie, just one element in each row is non-zero. The orthogonality relation is written:

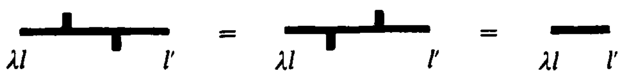

(16)

The phase $\phi_\lambda = \phi_{\lambda^*}$ produced by reflection may be written:

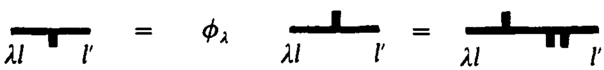

According to the Derome–Sharp lemma (B8.2)

(B8.2)
(S3.4)

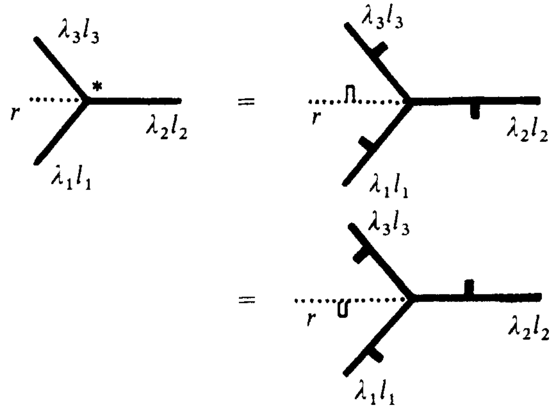

(17)

where a stub on a multiplicity line signifies the (real orthogonal) matrix $A(\lambda_1\,\lambda_2\,\lambda_3)_{rs}$ of (B8.2), with the usual anticlockwise convention. The second part of equation (17) follows from the first part, equation (16) and the orthogonality of $A(\lambda_1\,\lambda_2\,\lambda_3)_{rs}$. We shall ignore the stubs on multiplicity lines, since for many finite groups (including crystal point groups, Butler and King 1974) $A(\lambda_1\,\lambda_2\,\lambda_3)_{rs} = \delta_{rs}$; ie, we assume quasi-ambivalence.

Equations (3), (12) and (14) give that

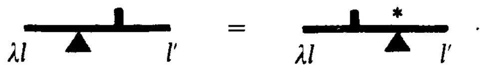

(18)

A loop with a stub has a simple value:

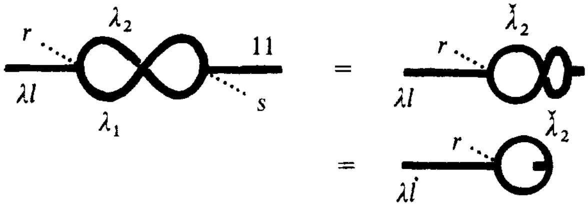

$= \delta_{\lambda 1}(\delta_{r1}\delta_{rs})\,.$ (19)

A Clebsch–Gordan coefficient (in Butler's (1974) 'sensible' phase convention, from which the R_3 convention unfortunately differs) is written

(B5.2)
(S3.7)

$\langle r\lambda l|\lambda_1 l_1, \lambda_2 l_2\rangle \;\leftrightarrow$ 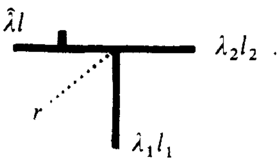

(20)

Using equations (16), (17) the complex conjugate coefficient is

$\langle \lambda_1 l_1, \lambda_2 l_2|r\lambda l\rangle \;\leftrightarrow$ 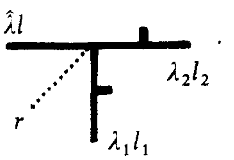

(21)

It is easy to verify the orthogonality relations for Clebsch–Gordan coefficients (B3.3, 3.4, 3.6) using these diagrams. We shall also need the results

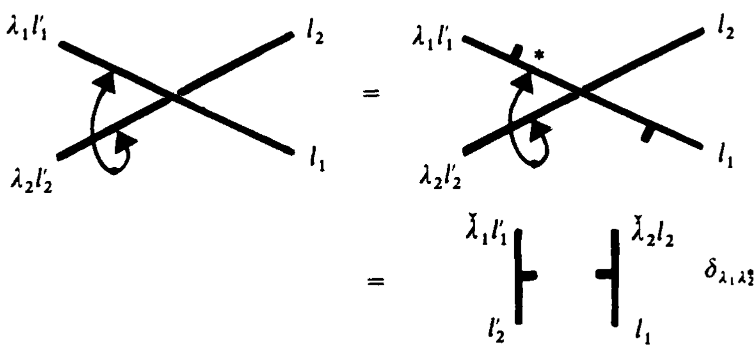

(22)

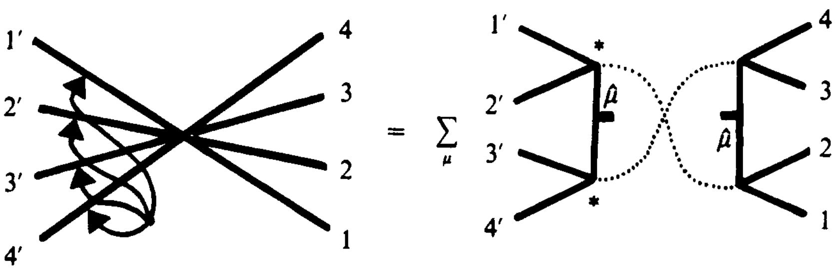

(23)

where i represents $\lambda_i l_i$, and i', $\lambda_i l'_i$. Equation (23) is proved by using equation (11) twice, and then equations (12), (22), on the left side.

3.3. *Permutation matrices*

As explained in § 7, the detailed manipulation of permutations is an unnecessary complication for many applications. However, a diagram technique can be valuable.

Let (abc) represent a permutation π of (123). The permutation matrix is defined by

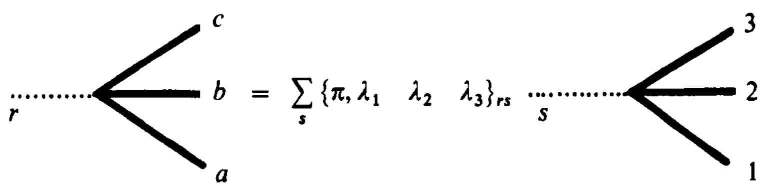

(24)

It follows that (using equation (9a))

$\{\pi, \lambda_1 \quad \lambda_2 \quad \lambda_3\}_{rs} \quad =$

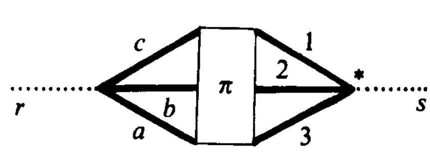

where the box labelled π signifies the necessary linkage. We obtain the particular values of table 1. Permutation matrices may be chosen to be real. Labels $\lambda_1\lambda_2\lambda_3$ need not be added since each multiplicity line must connect the same triple.

Table 1. Representation of 3-*jm* permutation matrices. The columns give the permutation π and the diagram form of $\{\pi, \lambda_1\ \lambda_2\ \lambda_3\}_{rs}$. These diagrams will be drawn on a smaller scale in the following.

(1)	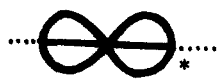
(12)	
(23)	
(13)	
(123)	
(132)	

3.4. n-j for n > 3

A 6-*j* symbol may be defined as

(B9.6)
(S5.2)
$$\begin{Bmatrix} \lambda_1 & \lambda_2 & \lambda_3 \\ \mu_1 & \mu_2 & \mu_3 \end{Bmatrix}_{r_1 r_2 r_3 r_4} \leftrightarrow \qquad (25)$$

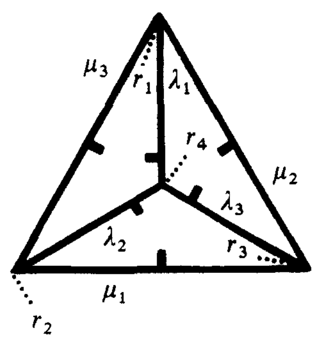

Note that the μ_i labels are in leading positions relative to the inward-pointing stubs. Diagram proofs of the various symmetries of the 6-*j* symbol (B9.7, 9.8, 9.9) represent simple exercises in permutation manipulations.

A 9-j symbol similarly becomes

(B10.2)
(S5.6)

$$\begin{matrix} \begin{Bmatrix} \lambda_1 & \lambda_2 & \lambda_3 \\ \mu_1 & \mu_2 & \mu_3 \\ \nu_1 & \nu_2 & \nu_3 \end{Bmatrix} & \begin{matrix} r_1 \\ r_2 \\ r_3 \end{matrix} \\ \begin{matrix} s_1 & s_2 & s_3 \end{matrix} & \end{matrix} \leftrightarrow$$

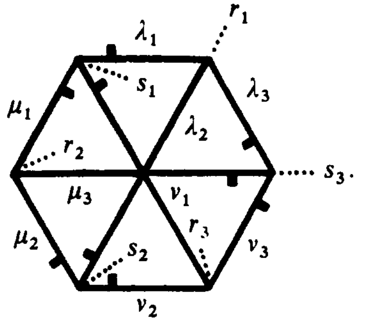

(26)

4. Jucys–Levinson–Vanagas theorems

As in § 3, it becomes natural to introduce a twisted version of the standard theorems when generalizing them for the inclusion of multiplicity lines.

4.1. Basic theorem

If a subdiagram A_n has n external solid lines (and any number of external multiplicity lines), consists of 3-jm vertices, and has one 2-jm symbol (stub) on each internal line, it is invariant under a group operation except for the external lines:

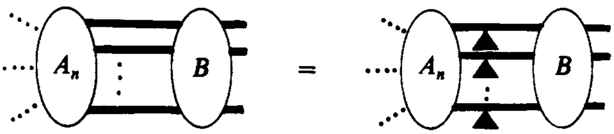

(27)

(any stubs on the n lines external to A_n are to be included in B).

Proof. Use equation (12) for each internal 3-jm, and note that each internal line has the form

Subsidiary Theorems. Perform a group integral, and then apply equations (6), (22), (13) and (23) to the basic theorem for $n = 1, 2, 3, 4$ respectively:

YLV 1:

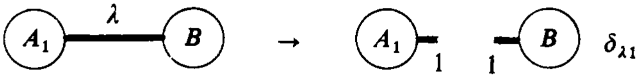

(28)

YLV 2:

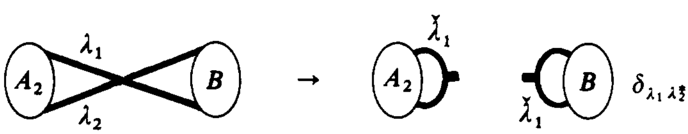

(29)

YLV 3: 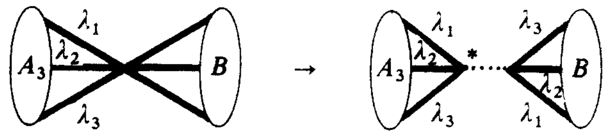 (30)

YLV 4: 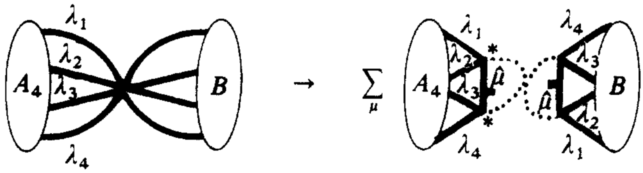 (31)

Note that in (31) any two 3-*jm*'s may be starred. Thus the YLV*n* theorems appear as the analogues of equation (11) for multiplicity lines.

For the groups in which we are interested, singlet representations $\lambda(|\lambda| = 1)$ are relatively common. If λ_1 is a singlet and $\lambda_2 = \lambda_1^*$, the phases $\lambda_1(g)_{11}\lambda_2(g)_{11}$ cancel, and we have special cases of equations (30), (31):

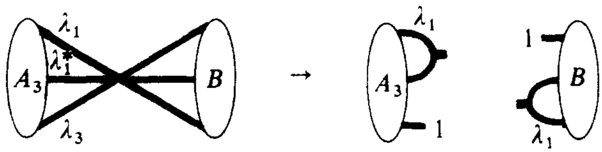 (32)

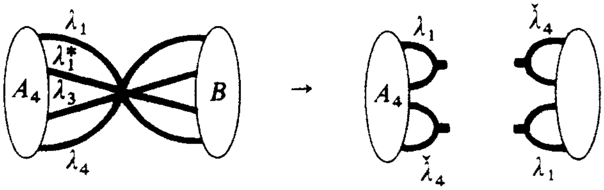 $\delta_{\lambda_3\lambda_3^*}$ (33)

Space permits of only one example of all preceding theory; we take the Racah back-coupling relation (B9.10), which illustrates 6-*j* symmetries, permutation matrices, YLV4 and all the more fundamental results. We compute the right side of (B9.10):

$$X = \sum_{\nu} |\nu|\phi_{\mu_2}\theta(\mu_1\lambda_2\mu_3^*r_2)\theta(\lambda_1\lambda_2\lambda_3r_4)\theta(\lambda_1\mu_1\nu^*r) \times \begin{Bmatrix} \lambda_2 & \lambda_1 & \lambda_3 \\ \mu_1 & \mu_2 & \nu \end{Bmatrix}_{r'rr_3r_4} \begin{Bmatrix} \lambda_1 & \mu_1 & \nu^* \\ \lambda_2 & \mu_2 & \mu_3 \end{Bmatrix}_{r_1r_2r'r}$$

$= \sum_{\nu r r'}$ 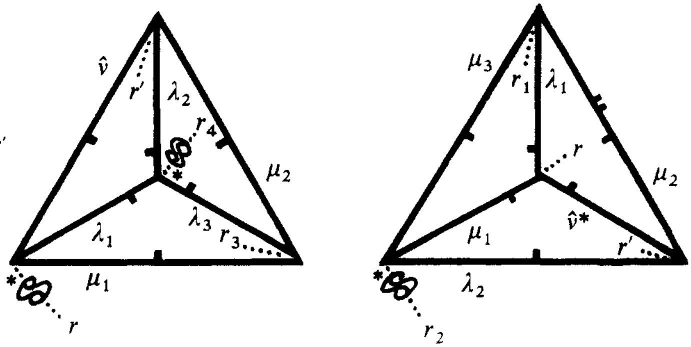

$= \sum_{\nu r r'}$ 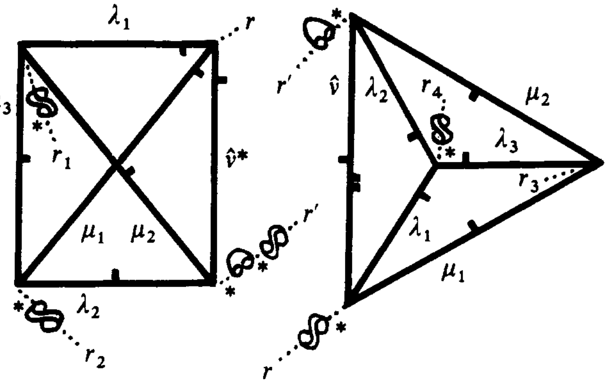

$= \sum_{\nu}$ 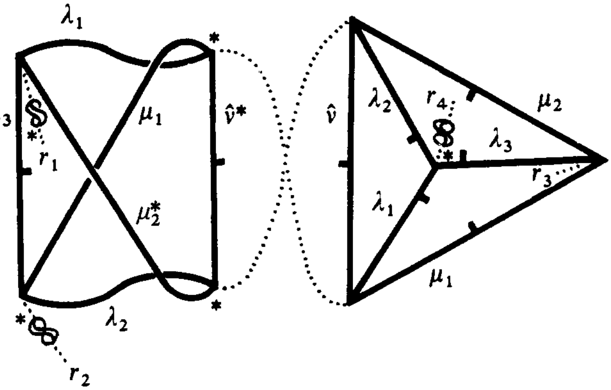

$\xrightarrow{\text{YLV 4}}$ 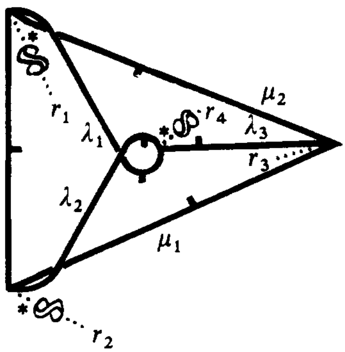

which equals the left side.

5. Tensor operators

We depict the matrix element of a tensor operator by

$\langle \lambda_1 l_1 | Q_l^{\lambda} | \lambda_2 l_2 \rangle \quad \leftrightarrow$ 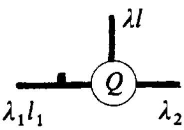 (34)

This asymmetric definition is used in order to ensure the following theorems.

Theorem 1. If Q_l^λ is an *irreducible tensor* operator, the box labelled Q is an *invariant* subdiagram.

Proof. Insert $O_g O_{g^{-1}}$ factors before and after Q_l^λ in the matrix element. Use $O_{g^{-1}}^+ = O_g$ to write out the effect on bra and ket explicitly; use the defining relation (B16.2) $O_g Q_l^\lambda O_{g^{-1}} = Q_{l'}^\lambda \lambda(g)_{l'l}$. Hence

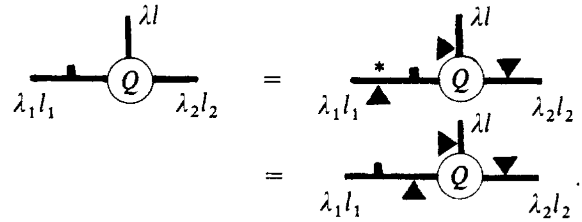

Applying YLV3, we obtain the Wigner–Eckart theorem (B16.4)

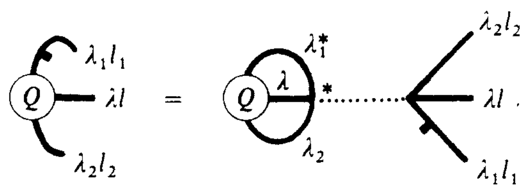

(35)

Unlike Sandars (1969), we find considerable value in this diagrammatic representation of a reduced matrix element, partly because of the multiplicity summation.

5.1. Conjugate operator

Under complex conjugation, equation (34) becomes

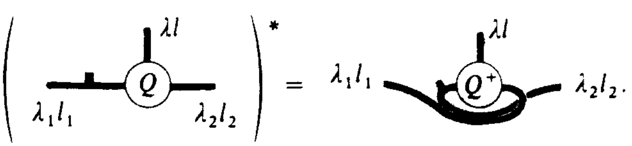

(36)

The asymmetry in equation (34) has the consequence that the box labelled Q^+ is not an invariant subdiagram, ie the Hermitian conjugate of an irreducible tensor operator is not a tensor operator. Instead we have the following theorem.

Theorem 2. If Q_l^λ is an irreducible tensor operator,

$$\tilde{Q}_{l'}^\lambda \equiv (Q_l^\lambda)^+(\lambda)_{ll'} \tag{37}$$

is also an irreducible tensor operator, conjugate to Q_l^λ.

Proof. From equation (36)

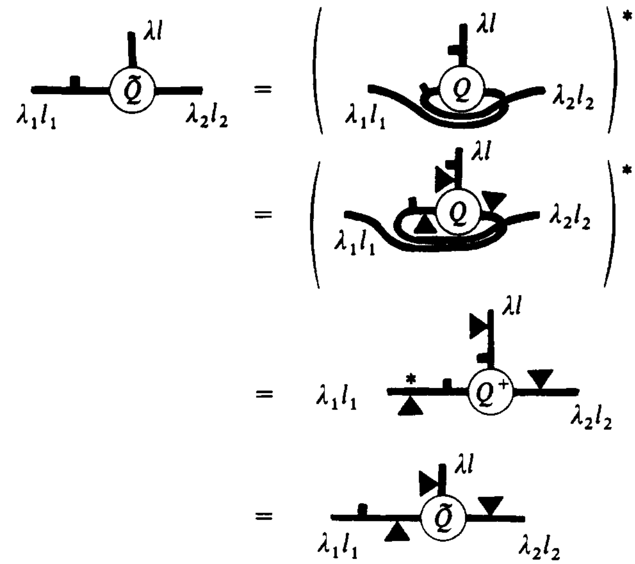

(38)

It has been known for some time (eg Judd 1967) that if the Hermitian conjugate of an R_3 tensor operator is to obey tensorial commutation relations, a phase $(-1)^{j-m}$ has to be included. This is just the R_3 counterpart of the 2-*jm* symbol introduced in equation (37). We note that the definition of a tensor annihilation operator in equation (14) of Wybourne (1973) should include the 2-*jm* symbol for the finite group under consideration (as well as the R_3 phase for the spin part) in order to be a double tensor.

It is a simple exercise in diagrams to obtain the relation between the reduced matrix elements of a tensor and its conjugate, using equations (35) and (38):

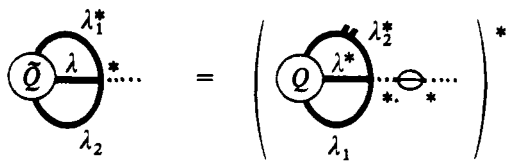

(39)

ie

$$\langle\lambda_1\|\tilde{Q}^{\lambda r}\|\lambda_2\rangle = \phi_{\lambda_2}\{(13)\lambda_2^*\lambda^*\lambda_1\}_{rs}\langle\lambda_2\|Q^{\lambda^* s}\|\lambda_1\rangle^*. \tag{39}$$

5.2. Coupled tensor operators

We write the matrix element of an operator product by inserting a complete set of states

$\langle P^{\kappa_1}_{k_1}Q^{\kappa_2}_{k_2}\rangle$ =

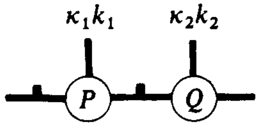

Using equation (21) we may couple the κ_i lines and still leave internal parts invariant, thus constructing a new tensor operator:

(B19.2) $\langle (P^{\kappa_1}_{k_1} Q^{\kappa_2}_{k_2})^{\kappa r}_{k} \rangle \leftrightarrow$

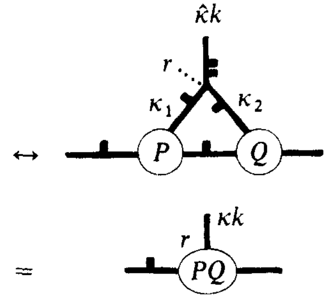

(40)

A straightforward application of equation (35) and YLV3 yields the relation between reduced matrix elements:

(B19.5)

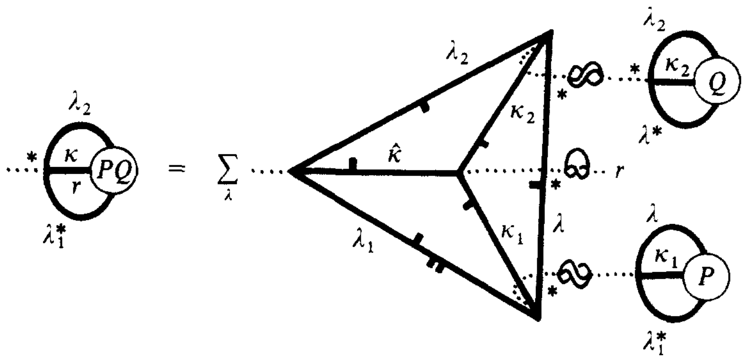

(41)

6. Application to Feynman diagrams

Consider first a perturbation involving three creation or annihilation operators (eg electron–photon, ion–phonon interaction):

$$H_i = \sum_{\mu m \nu n \kappa k} a^{\dagger}_{\mu m} a_{\nu n} (V_{\mu m,\nu n,\kappa k+} b^{\dagger}_{\kappa k} + V_{\mu m,\nu n,\kappa k-} b_{\kappa k}).$$

It is necessary for our purposes to distinguish the various coefficients V. $a^{\dagger}_{\mu m}$ creates a quasi-fermion in a state transforming as component m of irrep μ, etc. Since the vacuum is an invariant, $a^{\dagger}_{\mu m}$ is a tensor operator, $(a^{\dagger})^{\mu}_{m}$, and $b^{\dagger}_{\kappa k} = (b^{\dagger})^{\kappa}_{k}$. From equation (37), $(\tilde{a})^{\mu *}_{m'} \equiv a_{\mu m}(\mu)_{mm'}$ and $(\tilde{b})^{\kappa *}_{k'} \equiv b_{\kappa k}(\kappa)_{kk'}$ are the conjugate tensors. On substitution into the above equation we obtain

$$H_i = \sum_{\mu m \nu n n' \kappa k} \left((a^{\dagger})^{\mu}_{m} (b^{\dagger})^{\kappa}_{k} (\tilde{a})^{\nu *}_{n'} (\nu)_{nn'} V_{\mu m,\nu n,\kappa k+} + \sum_{k'} (a^{\dagger})^{\mu}_{m} (\tilde{b})^{\kappa *}_{k'} (\tilde{a})^{\nu *}_{n'} (\nu)_{nn'} (\kappa)_{kk'} V_{\mu m,\nu n,\kappa k-} \right).$$

However, H_i is also an invariant operator; the coefficients of the tensors must couple them into the identity representation. Using equation (40) repeatedly we find that a matrix element of H_i has the form (a box represents an arbitrary invariant diagram)

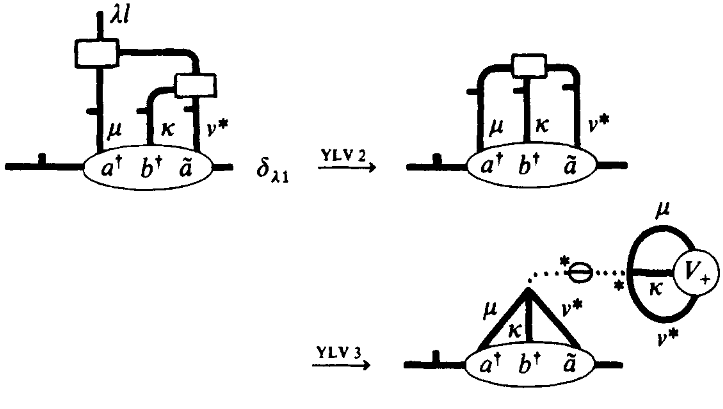

ie, the coefficients must be essentially a complex conjugated 3-*jm* symbol whose multiplicity index is summed with an arbitrary 'reduced matrix element' (cf the *jm* coefficients of Brink and Satchler 1968). Hence

$V_{\mu m,\nu n,\kappa k+}$ ↔ 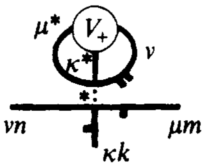 (42)

$V_{\mu m,\nu n,\kappa k-}$ ↔ 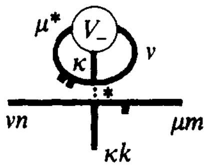 (43)

Since H_i is Hermitian, $V_{\mu m,\nu n,\kappa k+} = V^*_{\nu n,\mu m,\kappa k-}$ and therefore

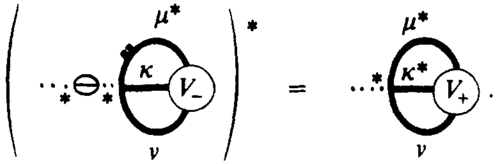 (44)

The 3-*jm* parts of equations (42) and (43) are topologically identical to the corresponding Feynman diagrams:

$V_{\mu m,\nu n,\kappa k+}$ ↔ 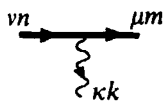 (45)

$V_{\mu m,\nu n,\kappa k-}$ ↔ 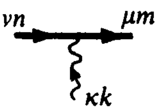 (46)

even to the extent that a 2-*jm* vertex on a 'creation' line corresponds to a Feynman arrow with the same sense as the angular momentum arrow of equation (15). It follows that each line internal to a Feynman diagram has one 2-*jm* vertex on it. We conclude (cf § 4) that the internal parts of a Feynman diagram are invariant, and that the transformation properties of such a diagram may be obtained by using the YLV *n* theorems on the free ends.

For four-operator interactions (eg nonlinear ion–phonon interaction) the correspondence necessitates some standard form of coupling. We could take, for example,

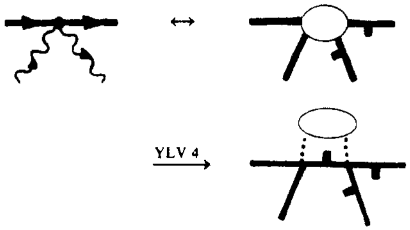

(47)

where boxes represent invariant diagrams. While exact isomorphism is not possible, the comments of the last paragraph continue to apply.

7. Simplifications for crystal point groups

If the group G is *simply reducible* ($n_{\lambda_1\lambda_2\lambda_3} \leqslant 1$ for all λ_i in G, cf § 3), the only modification to the standard R_3 diagrams that is necessary is the re-interpretation of the phase associated with any interchange permutation (use equation (9) where j_i is now a number permanently associated with λ_i (Butler 1974, Griffith 1962)). If, in addition, our 'twisted' versions of the standard diagrams are used, interchange phases are rarely needed.

A point group G may not be simply reducible (eg O, O_h, T = tetrahedral group, K = icosahedral group). If it is a *simple phase* group, that is, if

$$\sum_g [\chi^\lambda(g)]^3 = \sum_g \chi^\lambda(g^3):$$

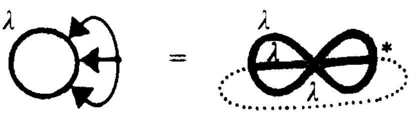

or (as an equivalent definition) **1** does not occur in the mixed (S_3) symmetry part of $\lambda \otimes \lambda \otimes \lambda$, for all λ in G (Butler 1974), cyclic permutations are invariance operations. If, in addition, a judicious choice of conventions is made, it may be possible for some simple phase groups (eg the tetrahedral group: Butler and Wybourne 1975) to make the interchange matrices diagonal and simply related to the R_3 phase of equation (9):

$$m\{\pi, \lambda_1 \quad \lambda_2 \quad \lambda_3\}_{rs} = \delta_{rs}(-1)^{j_1+j_2+j_3+r-1} \tag{48}$$

where j_i is a number permanently associated with λ_i; π = (12), (23) or (31). In this case the coupling systematics are very similar to those of R_3 (multiplicity lines and $\lambda \neq \lambda^*$ being the two chief differences) and our comments on simply reducible groups apply. We see, from the tables of Boyle (1972) that *all crystal point groups are simple phase.* However, if (*a*) it is not possible to satisfy equation (48); or (*b*) existing tabulations are not consistent with equation (48), and particularly if (*c*) intra-atomic coupling is analysed using such groups as R_7 or G_2 (which are not simple phase), our general formulation is required.

8. Conclusions

The diagram technique for angular momentum can be generalized to all compact groups. The main alterations necessary are the introduction of multiplicity lines and permutation matrices for non-simply reducible groups. 'Twisted' forms of the standard results prove easier to use in practical coupling calculations. The technique can be made particularly simple for simple phase groups. Isomorphism exists with Feynman diagrams, including the sense of the propagators. Internal parts of a Feynman diagram correspond to invariants; therefore, generalizations of the powerful general theorems of Jucys *et al* may be applied. The theoretical or experimental physicist who has some familiarity with the R_3 technique need learn very little additional material in order to employ the technique for compact groups.

As in the case of R_3, diagram techniques permit the elegant and rapid reduction of a complex problem to its group-theoretic essentials. In a following paper we will illustrate the technique in discussing lineshapes in a Jahn–Teller active system. The economy of the method is in striking contrast to the heavy algebra otherwise necessary in this example.

Acknowledgments

I am grateful to Professor B G Wybourne, Dr P H Butler and Dr D J Newman for their advice and encouragement.

References

Agrawala V K and Belinfante J G 1968 *Ann. Phys., NY* **49** 130–70
Briggs J S 1971 *Rev. Mod. Phys.* **43** 189–230
Brink D M and Satchler G R 1968 *Angular Momentum*, 2nd edn (London: Oxford University Press) chap 7
Boyle L L 1972 *Int. J. Quant. Chem.* **6** 725–46
Butler P H 1974 *Phil. Trans. R. Soc.* A **277** 545–85
Butler P H and King R C 1974 *Can. J. Math.* **26** 328–39
Butler P H and Wybourne B G 1975 *Int. J. Quant. Chem.* to be published
El-Baz E and Castel B 1972 *Graphical Methods of Spin Algebras* (New York: Dekker)
Griffith J S 1962 *The Irreducible Tensor Method for Molecular Symmetry Groups* (New Jersey: Prentice-Hall)
Harnung S E 1973 *Molec. Phys.* **26** 473–502
Judd B R 1967 *Second Quantization and Atomic Spectroscopy* (Baltimore: Johns Hopkins) p 32
Sandars P G H 1969 *Lectures in Theoretical Physics, Brandeis University Summer Institute*, vol 1 eds M Chrétien and E Lipworth (New York: Gordon and Breach) pp 171–216
Wybourne B G 1973 *Int. J. Quant. Chem.* **7** 1117–37